

Stabilization of the Vaterite Structure in the Presence Of Copper(II): Thermodynamic and Spectroscopic Studies

N. Nassrallah-Aboukaïs,[†] A. Boughriet,[‡] J. Laureyns,[§] L. Gengembre,[¶] and A. Aboukaïs^{*,||}

Laboratoire de Chimie Analytique et Marine, CNRS URA 1363, Université des Sciences et Technologies de Lille, 59655 Villeneuve d'Ascq, France, IUT Béthune, Department Chimie, Rue de l'Université, 62408 Bethune, Cedex, France, Laboratoire de Spectrochimie Infrarouge et Raman du CNRS, Centre d'Etudes et de Recherches Lasers et Applications, Université de Lille I, 59655 Villeneuve d'Ascq, Cedex, France, Laboratoire de Catalyse Hétérogène et Homogène, URA 402 CNRS, U.S.T.L (Lille I) 59655 Villeneuve d'Ascq, Cedex, France, and Laboratoire de Catalyse et Environnement, EA 2598, MREID, Université du Littoral-Côte d'Opale, 145 Route du Pertuis d'Amont, 59140 Dunkerque, France

Received May 12, 1998. Revised Manuscript Received October 5, 1998

The crystalline transformation of vaterite in the presence of copper(II) [Cu(II)] has been investigated in ultrapure water and at room temperature using several techniques; scanning electron microscopy (SEM), infrared (IR) and micro-Raman spectroscopy. Our findings show that a slowing down of this transformation occurs and is intimately related to the generation of CuCO_3 layers on CaCO_3 surfaces. This phenomenon is also accompanied by a decrease of vaterite solubility. All these observations have led us to suggest that these Cu(II) coatings prevent the dissolution of the metastable calcium carbonate, vaterite. To prove this suggestion, experiments on solubilities of Cu^{2+} -vaterite solids were performed and interpreted in terms of thermodynamic equilibrium and stoichiometric saturation concepts. Thermodynamic and spectroscopic data demonstrate that the apparent stabilization of vaterite in the presence of Cu(II) is strongly dependent on the existence of water molecules in the lattice of the solid solution $\text{Cu}_x\text{Ca}_{1-x}\text{CO}_3$ as $(\text{H}_2\text{O})_y\text{Cu}_x\text{Ca}_{1-x}\text{CO}_3$. The chemical composition of this complex has been determined by X-ray photoelectron spectroscopy and thermogravimetry. Thus, the free energy of formation of such hydrated Cu(II) complexes has been found to be slightly lower than that for calcite. However, for high Cu(II) concentrations, metallic multilayers cannot grow indefinitely, and malachite $[\text{Cu}_2(\text{OH})_2(\text{CO}_3)]$ appears as a new phase. SEM and micro-Raman techniques have allowed successfully monitoring these morphological phenomena/transformation.

Introduction

Some of the most interesting studies of carbonate mineral surfaces chemistry have been concerned with the interactions of metal ions with calcite and aragonite.¹ Indeed, these interactions are generally of most importance to an understanding of metal geochemistry. In addition, removal of certain metals with calcium carbonates from industrial wastewaters or exhausted gas may be considered as an easy and low-cost procedure to limit contamination in the immediate vicinity of some industries. However, these investigations have been performed in a much less systematic manner than those involving other mineral phases, such as clays and iron oxides/hydroxides. To clarify these complex mechanisms, they should be studied more exhaustively.

In this context, among the different crystalline forms of calcium carbonates, vaterite (an orthorhombic calcium carbonate structure) was chosen in the present work because it behaves in water like a metastable crystal to give calcite (a rhombohedral calcium carbonate structure)^{2–7} and can be synthesized in the form of micropellets with well-defined sizes and relatively high specific areas.

In recent works,^{8,9} it was shown that a slowing down of this crystalline transformation occurs in the presence of copper(II), and a stabilization of vaterite is further

* To whom correspondence should be addressed.

[†]Laboratoire de Chimie Analytique et Marine.

[‡]IUT Béthune.

[§]Laboratoire de Spectrochimie Infrarouge et Raman du CNRS.

[¶]Laboratoire de Catalyse Hétérogène et Homogène.

^{||}Laboratoire de Catalyse et Environnement.

(1) Morse, J. W.; Mackenzie, F. T. *Geochemistry of Sedimentary Carbonates*, Elsevier Science: The Netherlands, 1990; p 707.

(2) Bischoff, J. L. *Am. J. Sci.* **1968**, 266, 80.

(3) Albright, J. N. *Am. Mineral* **1971**, 56, 620.

(4) Turnbull, A. G. *Geochim. Cosmochim. Acta* **1973**, 37, 1593.

(5) Nakahara, Y.; Tazawa, T.; Miyata, K. *Nippon Kagaku Kaishi* **1976**, 5, 732.

(6) Yamaguchi, T.; Murakawa, K. *Zairyo* **1981**, 30, 856.

(7) Ogino, T.; Suzuki, T.; Sawada, K. *Geochim. Cosmochim. Acta* **1987**, 51, 2757.

(8) Nassrallah-Aboukaïs, N.; Boughriet, A.; Fischer, J. C.; Wartel, M.; Langelin, H. R.; Aboukaïs, A. *J. Chem. Soc., Faraday Trans.* **1996**, 92, 3211.

(9) Nassrallah-Aboukaïs, N.; Boughriet, A.; Laureyns, J.; Aboukaïs, A.; Fischer, J. C.; Langelin, H. R.; Wartel, M. *Chem. Mater.* **1998**, 10, 238.

observed even after washing vaterite grains ($\sim 2 \text{ g}/0.5 \text{ dm}^{-3}$) with a Cu^{2+} solution ($10^{-3} \text{ mol dm}^{-3}$) for several days. We have assumed that Cu(II) adsorption on carbonate surfaces is responsible for such a phenomenon. The reaction should, indeed, lead to the generation of $\ll \text{CuCO}_3 \gg$ multilayers and/or coatings that might stop the dissolution of spherical grains of vaterite.

In this context, the identification of these solid copper compounds generated at the surface of vaterite grains and knowledge of their solubility is of utmost importance in understanding their chemical properties and the implication on the slowing down of the vaterite \rightarrow calcite transformation. In what follows, experimental data on Cu(II)–vaterite systems are reviewed and interpreted in terms of thermodynamic equilibrium and stoichiometric saturation concepts.

Experimental Section

Preparation of Cu^{2+} –Vaterite Samples. CuCl_2 solutions (10^{-4} , 10^{-3} , and $10^{-2} \text{ mol dm}^{-3}$) in ultrapure water were added to a known amount of vaterite ($2 \text{ g}/0.5 \text{ dm}^{-3}$). This heterogeneous mixture was shaken at room temperature to obtain an homogeneous carbonate phase. The sample was then filtered at different lapses of time on a $0.45\text{-}\mu\text{m}$ Sartorius filter (cellulose nitrate membrane). Ultrapure water is prepared as follows: A Milli-Q Plus water purification system (Millipore) is currently used in our laboratory to provide up to $1.5 \text{ L}/\text{min}$ of ultrapure water on demand for chemical analysis and synthesis. A QPAK₂ purification pack (Millipore), pretreated by resin deionized water, is used for this compact Milli-Q Plus system; it contains a $0.5\text{-}\mu\text{m}$ prefilter to protect other purification media from colloidal, organic, bacterial, pyrogenic, and particulate contamination often entrained in water pretreated by a regenerated ion-exchange resin; this pack also contains activated carbon, nuclear-grade ion-exchange resin, and organex-Q organic scavenger mixture.

Subsequently, recovered Cu(II)–vaterite solids were directly analyzed by the following techniques.

Infrared (IR) Spectroscopy. IR spectra were recorded either on a Perkin-Elmer FTIR model 1600 spectrometer or a Bruker FTIR model Vector 22 spectrometer. Using the KBr pellet technique, 1.5 mg of solid was mixed with 120 mg of dried KBr, and the mixture was afterward pressed at a pressure of $10 \text{ tons}/\text{cm}^2$. It is worth noting that numerous IR experiments were previously performed on pure vaterite to show the stability of this metastable calcium carbonate under the effects of such a high pressure.

Thermogravimetric Analysis (TGA) Measurements. These analyses were carried out on a SETARAM apparatus model TGA 92.

Scanning Electron Microscopy (SEM). The SEM microphotographs of the Cu^{2+} –vaterite solids during their different phases of transformation were taken on a JEOL JSMT 330A microscope. Before analysis, each sample was ground to a fine powder that was suspended in water.

Raman Microscopy. A microRaman/microfluorescence confocal scanning spectrometer manufactured by DILOR (France) was used for microanalysis of Cu(II)–vaterite solids. A schematic diagram of the instrument for confocal microRaman analysis has been described previously.¹⁰ The microscope optics are directly attached to the vertically mounted Raman spectrometer. A color camera mounted on the top of the microscope is used to feed a signal to a video monitor and provides an optical view of the sample. One computer (model 486-DX33) pilots and controls the microRaman spectrometer,

Table 1. Thermodynamic Dissociation Constants Corresponding to the Species Involved in CuCl_2 –Vaterite– H_2O Systems^a

dissolved species	log <i>K</i>	dissolved species	log <i>K</i>
" H_2CO_3 "	16.68	$\text{Cu}(\text{CO}_3)_2^{2-}$	9.83
HCO_3^-	10.33	CuOH^+	−8.00*
CaOH^+	−12.60* ^b	$\text{Cu}(\text{OH})_2 \text{ aq.}$	−13.68*
CaHCO_3^+	11.33	CuHCO_3^+	13.00
$\text{CaCO}_3 \text{ aq.}$	3.15	CuCl^+	0.43
$\text{Cu}_2(\text{OH})_2^{2+}$	−10.36*	$\text{CuCl}_2 \text{ aq.}$	0.16
$\text{Cu}(\text{OH})_3^-$	−26.90*	CuCl_3^-	−2.29
$\text{Cu}(\text{OH})_4^{2-}$	−39.60*	CuCl_4^{2-}	−4.59
		$\text{CuCO}_3 \text{ aq.}$	6.73

solid species	log <i>K</i>	solid species	log <i>K</i>
$\text{Cu}(\text{OH})_2$	−8.64*	ténorite	−7.62*
CuCO_3	9.63	calcite	8.48
malachite	5.18*	azurite	16.92

^a $X_n Y_m \rightleftharpoons n X^{m+} + m Y^{n-}$. ^b (*) Indicates equilibrium constants for hydroxide species as $X(\text{OH})_n + n \text{H}^+ \rightleftharpoons X^{n+} + n \text{H}_2\text{O}$.

and another one (RISC, 6000 IBM workstation) drives the data acquisition and displays microRaman spectra.

X-ray Photoelectron Spectroscopy (XPS) Measurements. The XPS spectra were obtained on a Leybold-Heraeus LHS 10 spectrometer equipped with an AlK α anticathode ($h\nu = 1486.6 \text{ eV}$). The spectra were recorded in a high vacuum (10^{-9} Torr). Binding energies were determined using the carbon 1s peak (from in situ contamination) at 285 eV for standardization. To evaluate the $n(\text{at.1})/n(\text{at.2})$ ratio of the atomic composition of the two atoms at.1 and at.2 present on the surfaces of powders recovered from the reaction $\text{Cu}^{2+} + \text{vaterite}$ in ultrapure water, the mathematical expression established by Larson¹¹ (valid for thin powders with infinite thickness) was used:

$$\frac{I_p(\text{at.1})}{I_p(\text{at.2})} = \frac{n(\text{at.1}) \cdot \sigma(\text{at.1}) \lambda(\text{at.1}) \cdot \text{Tr}(\text{at.1})}{n(\text{at.2}) \cdot \sigma(\text{at.2}) \lambda(\text{at.2}) \cdot \text{Tr}(\text{at.2})}$$

where $I_p(\text{at.1})$ and $I_p(\text{at.2})$ represent the areas of the photoelectron peaks of the elements at.1 and at.2, σ corresponds to the photoelectron cross section of the analyzed sample (which is taken from the Scofield tables¹²), λ is the escape depth of the photoelectron (which depends on the kinetic energy,¹³ E_k), and Tr represents the transmission factor of the analyzer (which is inversely proportional in our case, to the kinetic energy).

Elemental Analysis. The mixtures of Cu(II) + vaterite were filtered at different reaction times through $0.45\text{-}\mu\text{m}$ Sartorius filters (cellulose nitrate membrane). The recovered solids were attacked with a concentrated HCl solution ($\sim 1\text{--}3 \text{M}$). The Ca and Cu concentrations in the acidified liquid and solid phases were determined directly by means of inductively coupled plasma atomic emission spectroscopy (ICP-AES; ARL model 3510). Using an automatic pH titration (Metrohm; model SET/MET 702), pH potentiometric analyses of nonacidified liquid phases were carried out by adding a titrated solution of HCl ($5 \times 10^{-4}\text{--}10^{-3} \text{ mol dm}^{-3}$) under a nitrogen atmosphere. This titration allowed assessment of the total amount of dissolved inorganic carbon (i.e., $\ll \text{H}_2\text{CO}_3 \gg$, HCO_3^- , and CO_3^{2-}) in chemical equilibrium with the solid phase (calcium carbonate) under the influence of Cu(II).

Computation of the Distribution of Dissolved Species. The use of the MINEQL⁺ computer program¹⁴ has enabled us to calculate the concentrations of the different complexes obtained from the filtration of the various Cu(II)–vaterite

(10) Sharonov, S.; Chourpa, I.; Valisa, P.; Fleury, F.; Feofanov, A.; Manfait, M. *Eur. Microsc. Anal.* **1994**, 23.

(11) Larson, P. E. *J. Electron Spectrosc. Relat. Phenom.* **1979**, 4, 213.

(12) Scofield, J. H. *J. Electron Spectrosc. Relat. Phenom.* **1976**, 8, 129.

(13) Penn, D. R. *J. Electron Spectrosc. Relat. Phenom.* **1976**, 9, 29.

(14) Schecher, W. D.; McAvoy, D. C. *MINEQL⁺: A Chemical Equilibrium Program for Personal Computers*; Proctor and Gamble Company, 1994.

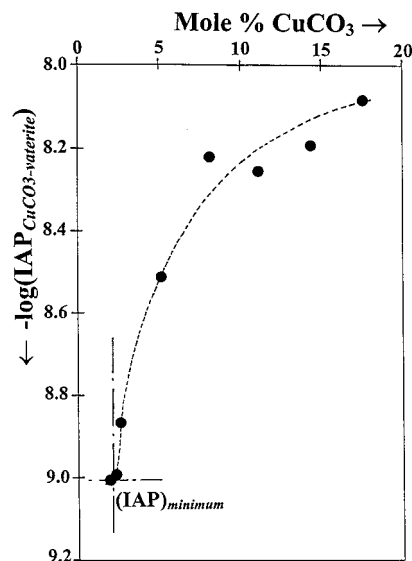


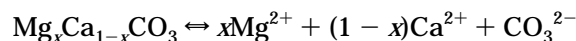
Figure 1. Variation of the stoichiometric activity product (IAP) as a function of the molar percentage of CuCO_3 generated at the surface of vaterite grains in Cu(II) –vaterite– H_2O systems after a reaction time of 1 day [vaterite: 4×10^{-2} M; Cu(II) : 10^{-2} – 10^{-4} M].

systems in ultrapure water (at chemical equilibrium and room temperature) after being analyzed by the ICP-AES technique. For that purpose, the thermodynamic constants corresponding to the interactions of the cations Ca^{2+} , Cu^{2+} , and H_3O^+ with inorganic ligands (OH^- , Cl^- , HCO_3^- , and CO_3^{2-}) have been taken into account (see Table 1).

Results and Discussion

Solubilities and Thermodynamic Properties.

Solubilities of magnesian calcites have been reported in numerous studies^{15,16} where the authors have assumed the existence of solid solutions $\text{Mg}_x\text{Ca}_{1-x}\text{CO}_3$, and their dissolution in aqueous solutions is described as follows:



They used an ionic activity product (IAP), which is defined as

$$\text{IAP}_{\text{Mg-calcite}} = (\text{Mg}^{2+})^x (\text{Ca}^{2+})^{1-x} (\text{CO}_3^{2-})$$

where (Mg^{2+}) , (Ca^{2+}) , and (CO_3^{2-}) represent the activities of the free ionic species Mg^{2+} , Ca^{2+} , and CO_3^{2-} , respectively.

The product just mentioned is also still called a stoichiometric solubility product. It is now considered as the most commonly used expression for solubility. Numerous authors^{15,17} have shown that the term $-\log \text{IAP}_{\text{Mg-calcite}}$ reaches a minimum value when the mol % of MgCO_3 is ca. 2–4%. The general trend of their experimental results indicates a decrease of solubility and/or a better thermodynamic stabilization of $(\text{MgCO}_3)_x\text{CaCO}_3$ systems. We have observed a similar phenomenon of thermodynamic stabilization in the case of

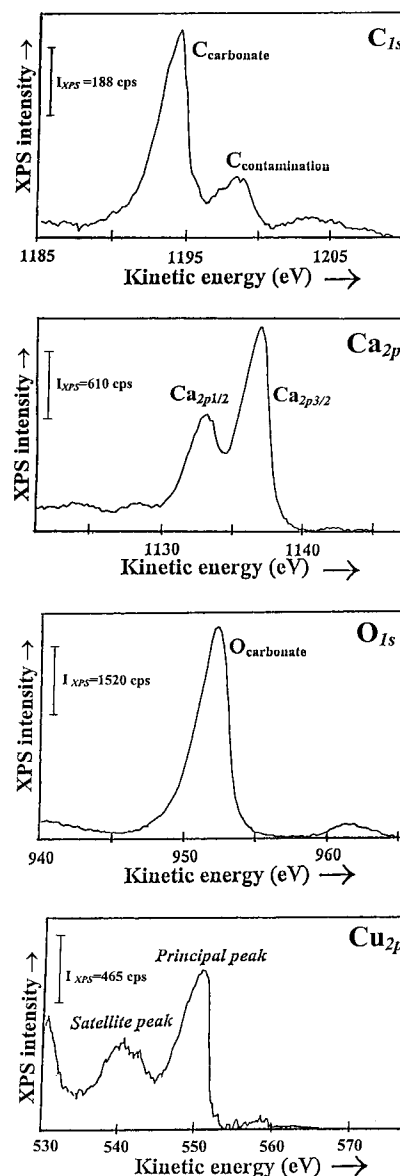
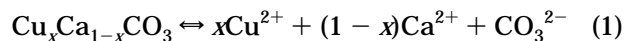


Figure 2. XPS spectra of C_{1s} , O_{1s} , Ca_{2p} and Cu_{2p} obtained for solids recovered from a mixture of vaterite (4×10^{-2} M) + CuCl_2 (8.7×10^{-4} M) after a reaction time of 1 day.

Cu(II) (10^{-3} M)–vaterite (4×10^{-2} M) systems in ultrapure water (where the vaterite structure remained stable after a reaction time of 4 days).⁹ To understand this phenomenon, we have tried to assess the stoichiometric solubility product IAP of the solid solution generated at vaterite surfaces during the course of the vaterite + Cu(II) reaction. For that purpose, the dissolution reaction described by the equilibrium



has been investigated in ultrapure water under aerated conditions by adding vaterite (4×10^{-2} M) to Cu(II) solutions (with Cu^{2+} concentrations varying from 10^{-4} to 10^{-2} M). The obtained liquid and solid phases of Ca and Cu were analyzed by ICP-AES. A pH-automatic titrator was used to determine the total dissolved inorganic carbon, under nitrogen atmosphere, by adding a dilute HCl solution (5×10^{-4} – 10^{-3} M) to a known volume of the filtered reaction mixture (50–150 mL).

(15) Mackenzie, F. T.; Bischoff, W. D.; Bishop, F. C.; Loijens, M.; Schoonmaker, J.; Wollast, R. *Reviews in Mineralogy*, Vol. 11; Carbonates: Mineralogy and Chemistry; Reeder, R. J., Ed.; Ribbe, P. H., Series Ed.; Mineralogical Society of America: 1983; p 97.

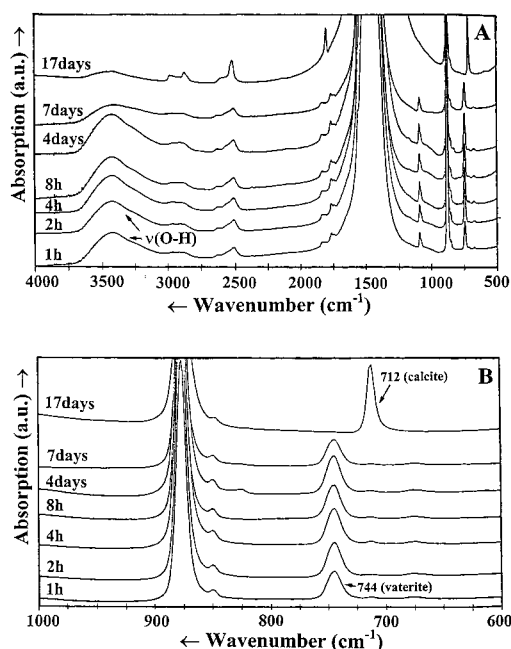
(16) Mucci, A.; Morse, J. W. *Rev. Aquatic Sci.* **1990**, 3, 217.

(17) Thorstenson, D. C.; Plummer, L. N. *Am. J. Sci.* **1977**, 277, 1203.

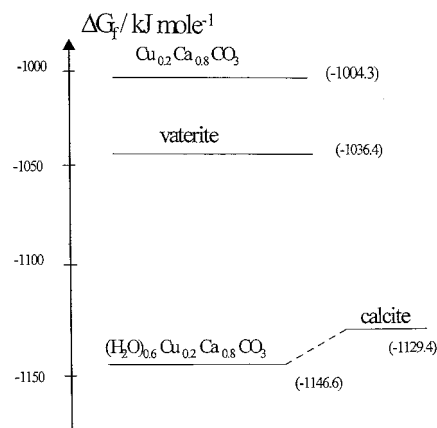
Table 2. Evolution versus Time of the XPS Parameters Obtained for the Atoms C_{1s}, O_{1s}, Ca_{2p}, and Cu_{2p_{3/2}} Present at the Surface of Copper(II)-Doped Vaterite^a

Part A						
compound	reaction time, days	C _{1s} ^b	O _{1s} ^b	Ca _{2p} ^b	Cu _{2p} ^b	$I_{\text{sat}}/I_{\text{pp}}$ for adsorbed copper ^c
vaterite		289.6 (2.1) ^d	531.4 (2.4) ^d	347.0 (2.3) ^d		
solids recovered from a mixture of vaterite (4×10^{-2} M) + Cu ²⁺ (8.7×10^{-4}) in ultrapure water	1	289.8 (2.1)	531.6 (2.4)	347.0 (2.3)	934.8 (3.6)	0.78
	4	289.9 (2.2)	531.7 (2.4)	347.2 (2.2)	934.5 (4.4)	0.62
Part B						
reaction time, days	$I(\text{O})/I(\text{Ca})^*$	$n(\text{O})/n(\text{Ca})$	$I(\text{Cu})/I(\text{Ca})$	$n(\text{Cu})/n(\text{Ca})$	$n(\text{Cu})/n(\text{Cu}) + n(\text{Ca})$	
1	1.80	3.35	0.97	0.25	0.20	
4	1.84	3.43	0.95	0.24	0.19(3)	

^a Copper(II): 8.7×10^{-4} M; vaterite: 4×10^{-2} M in ultra-pure water. ^b The XPS peaks of C_{1s}, O_{1s}, Ca_{2p}, and Cu_{2p_{3/2}} are referred to the carbon 1s photopeak, due to adventitious carbon, which appears at 285 eV. The binding energies are expressed in electrovolts, with an experimental error of 0.2 eV. ^c I_{sat} : satellite photoelectron peak; I_{pp} : principal photoelectron peak. ^d $\langle \rangle$: full-width-at-half-maximum (FWHM), in eV.

**Figure 3.** Evolution versus time of the IR spectra observed for solids recovered (after filtration) from a mixture of vaterite (4×10^{-2} M) + CuCl₂ (10^{-3} M) in ultrapure water.

The MINEQL⁺ computer program for the calculation of chemical equilibrium compositions of aqueous systems has been used, taking into account the concentration of total dissolved Ca, Cu, and inorganic C, the various equilibrium constants involved in the Cu(II)–vaterite system (Table 1),^{18–23} the pH of the reaction medium (pH = 7.4–7.8), and the pressure of carbon dioxide ($P_{\text{CO}_2} = 10^{-3.5}$ atm). These computer calculations

**Figure 4.** Energetic diagram, ΔG_f , representing the free energies of formation of the different carbonate precipitates involved in Cu(II)–vaterite–H₂O systems.

have allowed us to determine the concentrations of the different dissolved species present in the medium. From these results, we then calculated the stoichiometric activity products (IAP) for different concentrations of Cu(II) (varying from 10^{-4} to 10^{-2} M) in interaction with vaterite and plotted them against the mol% of CuCO₃ (Figure 1). The general trend of our experimental solubility data indicates that when [Cu²⁺] decreases, the calculated IAP value diminishes sharply to reach, finally, a minimum at IAP = 10^{-9} and mol% CuCO₃ = 2.1 (this result corresponds to an initial mixture of vaterite + Cu(II) of 4×10^{-2} M: 8.7×10^{-4} M). This thermodynamic behavior indicates that the solid solution Cu_xCa_{1-x}CO₃ can be treated as a new phase thoroughly coating vaterite grains, which is consequently responsible for the apparent decrease of the vaterite solubility. Under these conditions, we subsequently attempted to evaluate the equilibrium constant for reaction 1 when the stoichiometric solubility product for Cu(II)–vaterite systems reaches its lowest value, (IAP)_{min}, as shown in Figure 1. In this context, XPS, which is nowadays considered as one of the best techniques for surface analysis of solid materials,^{24,25} was used to determine the chemical composition of <<

(18) Weast, R. C.; Astle, M. V. *CRC Handbook of Chemistry and Physics*, 62nd ed.; CRC: Boca Raton, FL, 1981–1982.

(19) Michard, G. *Equilibres chimiques dans les eaux naturelles*; Publisud: 1989; p 357.

(20) Stumm, W.; Morgan, J. J. *Aquatic Chemistry: An Introduction Emphasizing Chemical Equilibria in Natural Waters*; Wiley and Sons: New York, 1981; p 780.

(21) Morel, F. M. M. *Principles of Aquatic Chemistry*; Wiley and Sons: New York, 1983; p 446.

(22) Smith, R. M.; Martell, A. E. *Critical Stability Constants: Inorganic Complexes*, Vol. 4; Plenum: New York, 1970.

(23) Baesjpi, C. F.; Mesmer, R. E. *The Hydrolysis of Cations*; Wiley: New York, 1976.

(24) D'Huysser, A., Thèse de doctorat. USTL (Lille I), 1982, p 130.

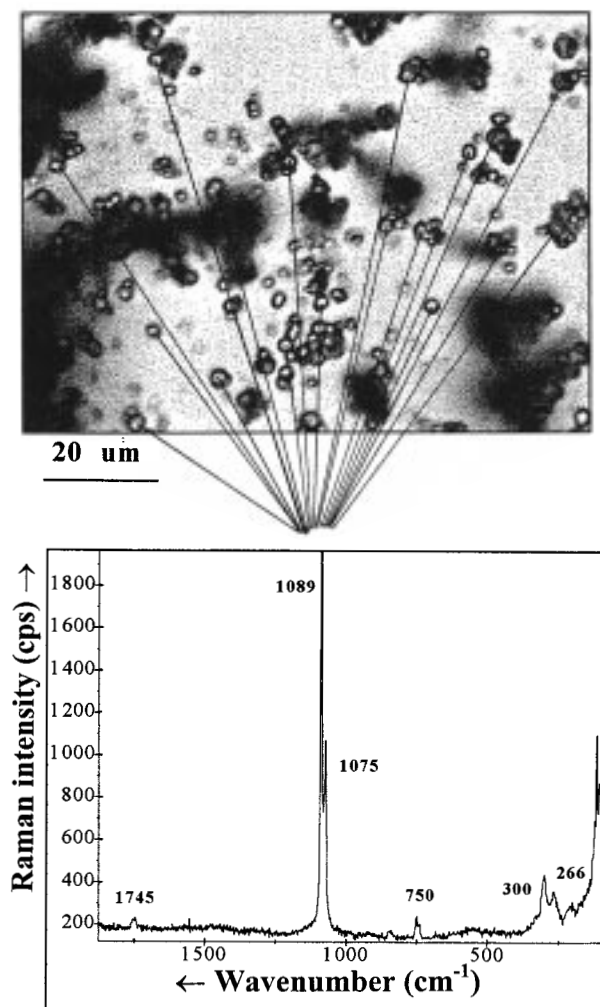


Figure 5. Micro-Raman spectrum of vaterite crystals stabilized with « copper coatings » obtained by washing vaterite ($4 \times 10^{-2} \text{ mol} \cdot \text{dm}^{-3}$) with a $10^{-3} \text{ mol} \cdot \text{dm}^{-3} \text{ CuCl}_2$ solution for 1 day. The optical microphotograph of Cu–vaterite grains recovered is also shown.

coatings » generated at the surface of the vaterite grains. Figure 2 represents the XPS spectra of O_{1s} , C_{1s} , Ca_{2p} , and Cu_{2p} obtained for the recovered solids after filtration from a mixture of vaterite ($4 \times 10^{-2} \text{ M}$) + Cu(II) ($8.7 \times 10^{-4} \text{ M}$) for a reaction time of 1 day. XPS data are summarized in Table 2. The mean chemical atomic stoichiometry $n_{\text{Cu}}/n_{\text{Ca}}$ of the outer layers (in depth, $\sim 75 \text{ \AA}$) evaluated from the quantitative analysis of the XPS spectra (as described in the Experimental Section) gave a $\text{Cu}_{0.2}\text{Ca}_{0.8}\text{CO}_3$ -like compound. The thickness of a such Cu(II) coating formed on the surface with the available Cu^{2+} quantity in solution was evaluated to 24 \AA ; that is, less than the analyses depth. Therefore, the coating thickness should be less than this theoretical value with a higher Cu content.

Taking into account the results just presented and the concentrations of the free dissolved ions Ca^{2+} , Cu^{2+} , and CO_3^{2-} (which were determined by undertaking a chemical speciation of the various species involved in the liquid phase using the MINEQL⁺ computational procedure as pointed out in the Experimental Section),

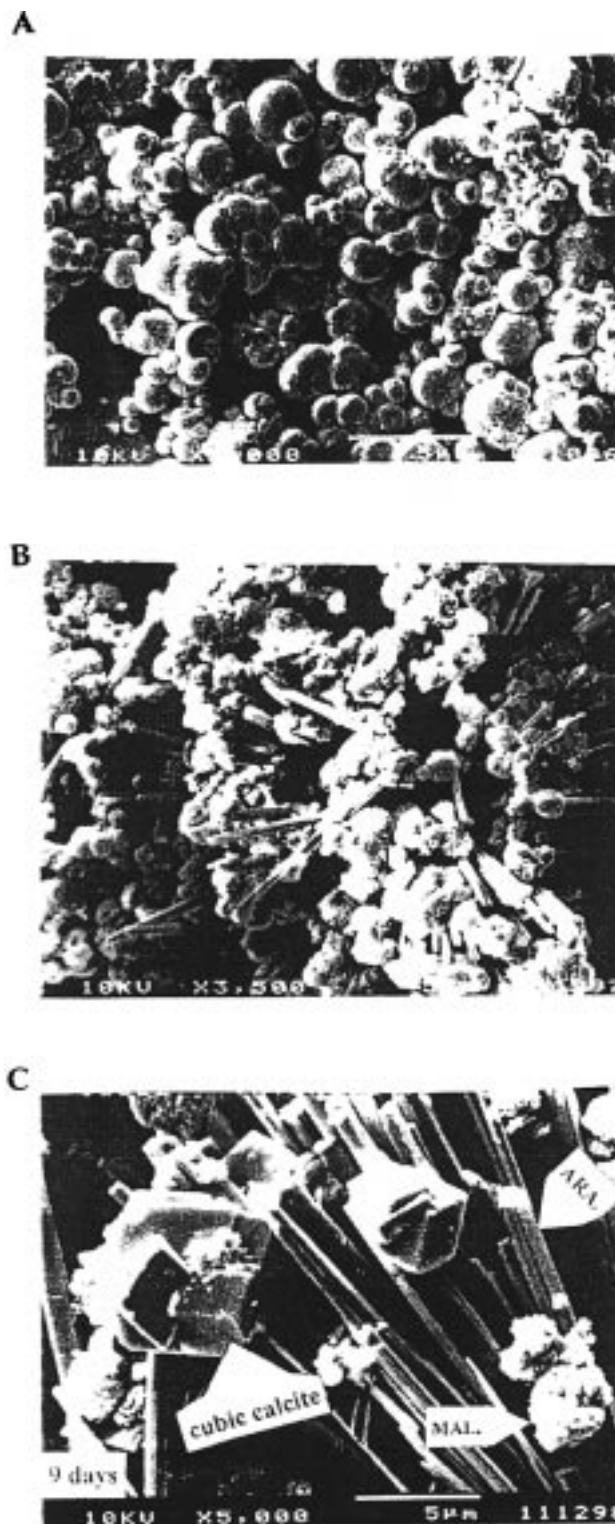


Figure 6. SEM microphotographs taken after washing vaterite ($4 \times 10^{-2} \text{ M}$) with (A) a 10^{-3} M CuCl_2 solution for 1 day and (B) for 7 days; and (C) with a 10^{-2} M CuCl_2 solution for 9 days (see ref 8) [vaterite: spherical micropellets; aragonite: needlelike structures; malachite: small (and mostly amorphous) particles deposited on other phases; cubic calcite: rhombohedral crystals].

the equilibrium constant for reaction 1 was calculated as $K(1) = 6.08 \times 10^{-9}$. The free energy of formation of the solid solution $\text{Cu}_{0.2}\text{Ca}_{0.8}\text{CO}_3$ can then be evaluated from the $K(1)$ value and the free energies of formation $\Delta_f G$ of the different dissolved species involved and which

(25) Briggs, D.; Seah, N. P. In *Practical Surface Analysis*, Second Ed., vol. 1, *Auger and X-ray Photoelectron Spectroscopy*; Wiley: Chichester, U.K. 1990.

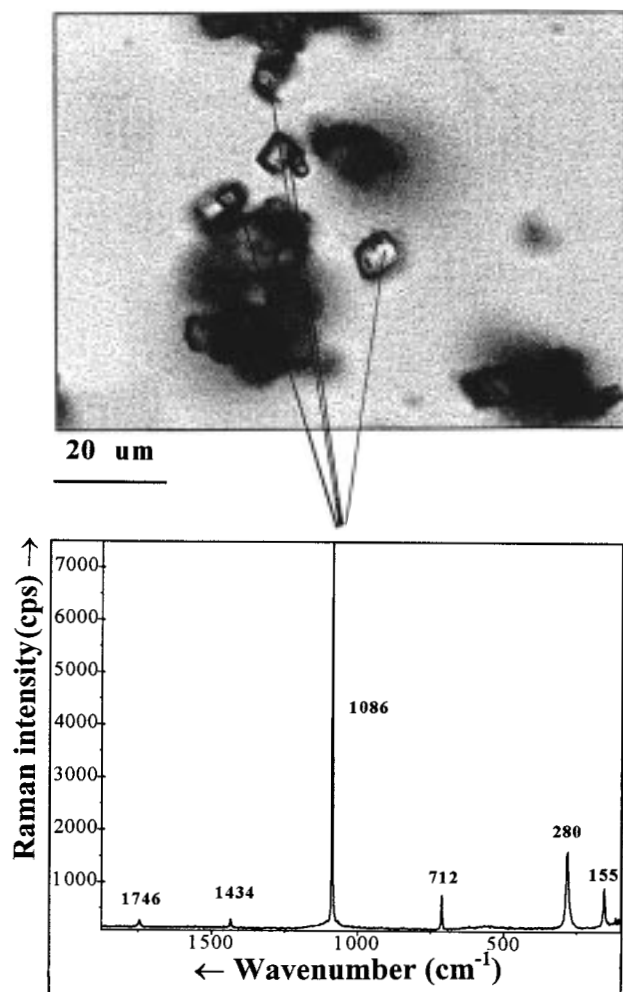


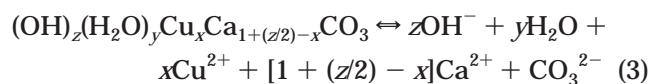
Figure 7. Micro-Raman spectrum of cubic calcite crystals (randomly selected) obtained after 4 days during the crystal-line vaterite (4×10^{-2} M) transformation in the presence of Cu(II) (10^{-3} mol·dm $^{-3}$). The optical microphotographs of the Cu-vaterite grains recovered is also shown.

are reported in the literature^{18,19} by the following equation:

$$\Delta_f G(\text{Cu}_x\text{Ca}_{1-x}\text{CO}_3) = x \Delta_f G(\text{Cu}^{2+}) + (1-x) \Delta_f G(\text{Ca}^{2+}) + \Delta_f G(\text{CO}_3^{2-}) + RT \ln[K(1)] \quad (2)$$

The value found for $\Delta_f G(\text{Cu}_x\text{Ca}_{1-x}\text{CO}_3)$ is equal to -1004 kJ. This value is nevertheless relatively higher than that for calcite [$\Delta_f G(\text{calcite}) = -1129$ kJ] and vaterite [$\Delta_f G(\text{vaterite}) = -1036$ kJ]. Consequently, we believe that the possible presence of water and/or hydroxide ions in the structure of this solid solution should affect its free energy of formation and thus its solubility. Indeed, it was shown previously that the introduction of water molecules or hydroxyl groups into the lattice of magnesian calcites¹⁵ or in the composition of compounds,²⁷ such as $[\text{Mg}(\text{OH})_2]$ brucite, $[\text{MgCO}_3 \cdot 3\text{H}_2\text{O}]$ nesquehonite, $[\text{Mg}_2(\text{OH})_2\text{CO}_3 \cdot 3\text{H}_2\text{O}]$ artinite, and $[\text{Mg}_5(\text{OH})_2(\text{CO}_3)_4 \cdot 4\text{H}_2\text{O}]$ hydromagnesite should be responsible for an increase in the heat of dissolution of

these hydrated structures and a diminution of their free energies of formation. In our case, a « shoulder » observed on the asymmetric XPS peak of O_{1s} (Figure 2), which is in the range of binding energies for O_{1s} atoms in H_2O and/or OH , suggests the existence of such a hydrated structure. It is interesting to note that before XPS analysis the Cu(II)-vaterite solid sample was treated under a vacuum of 10^{-6} – 10^{-7} mmbar at room temperature in the “preparation chamber” of the XPS apparatus for 15 min to eliminate all H_2O molecules that are not complexed with Cu(II) of vaterite grains. After the vacuum treatment, the XPS spectrum was recorded in the “analysis chamber” in a vacuum of 10^{-8} – 10^{-9} mmbar. Evidence supporting the hypothesis of hydrated Cu(II) complexes on vaterite surfaces has also been obtained by the IR spectroscopic studies of the Cu(II)-doped vaterite samples. Indeed, after drying the recovered solids for 4 days inside a laminar-flow hood (class 100 clean air) at room temperature, a bluish-colored powder is obtained [indicating the presence of hydrated Cu(II) complexes], and a strong absorption band corresponding to the stretching of the O–H bond can be still observed with a maximum near 3450 ± 5 cm^{-1} (Figure 3). The possibility of the presence of complexes such as $(\text{OH})_z(\text{H}_2\text{O})_y\text{Cu}_x\text{Ca}_{1+(z/2)-x}\text{CO}_3$ generated at the surface of the vaterite grains is sustained because Cu(II) is well-known to be a complexing ion,²⁸ particularly in natural compounds²⁹ with hydration properties,^{20,21} as well. In this case, the dissolution reaction becomes



and its equilibrium constant is given by the mathematical expression

$$K(3) = K(1)a_{\text{Ca}^{2+}}^{z/2}K_w^{z/2}a_{\text{H}^+}^z \quad [\text{or}] \quad \text{p}K(3) = \text{p}K(1) + z\text{p}K_w - z\text{pH} - z/2 \log(a_{\text{Ca}^{2+}})$$

where a_{H^+} and $a_{\text{Ca}^{2+}}$ represent the activity of H^+ and Ca^{2+} and K_w is the water ionic dissociation constant. The free energy of formation can be determined from the following equation

$$\Delta G^*[\text{Cu-complex}] = z\Delta_f G(\text{OH}^-) + y\Delta_f G(\text{H}_2\text{O}) + x\Delta_f G(\text{Cu}^{2+}) + [1 + (z/2) - x]\Delta_f G(\text{Ca}^{2+}) + \Delta_f G(\text{CO}_3^{2-}) + RT \ln[K(3)]$$

From its numerical expression given by

$$\Delta G^*[\text{Cu-complex}] \sim -1004 - 237y - 131z \quad (4)$$

(that is determined for $\text{pH} = 7.9$, $\text{p}K_w = 14$, and $[\text{Ca}^{2+}] = 1.5 \times 10^{-3}$ mol dm $^{-3}$), we undoubtedly can prove that the presence of water molecules and/or hydroxyl groups as ligands in the complexes contributes to a decrease of their free energy of formation. To determine whether the real $\Delta G^*[\text{Cu-complex}]$ value calculated for the Cu(II)-vaterite system is lower than/or close to the free

(26) Nassrallah-Aboukaïs, N.; Boughriet, A.; Gengembre, L.; Aboukaïs, A., unpublished results.

(27) Robie, R. A.; Hemingway, B. S.; Fischer, J. R. *U. S. Geol. Surv. Bull.* **1978**, 1452.

(28) Irving, H.; Williams, R. J. P. *J. Chem. Soc.* **1953**, 3192.

(29) Sparks, D. L. *Environmental Soil Chemistry*; Academic: New York, 1995.

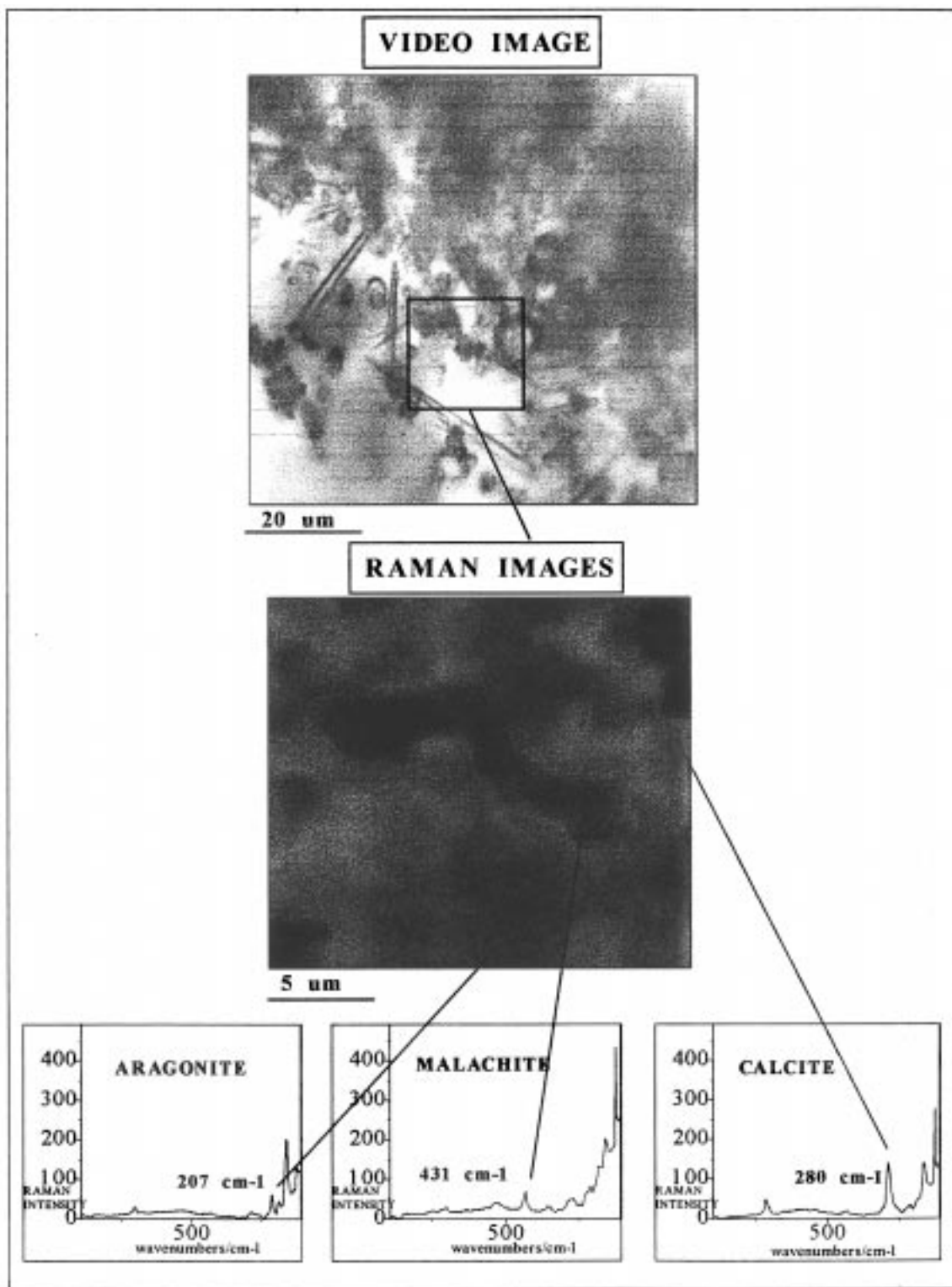
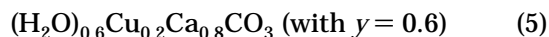


Figure 8. The optical microphotograph of Cu-vaterite grains recovered after washing vaterite ($4 \times 10^{-2} \text{ mol} \cdot \text{dm}^{-3}$) with a $10^{-2} \text{ mol} \cdot \text{dm}^{-3}$ CuCl_2 solution for 9 days and its Raman image decomposed into three components.

energy of formation of calcite it has been necessary to determine the y and/or z values. Using thermogravimetry, the amount of water associated with $\ll \text{Cu(II)-CuCO}_3 \gg$ complexes has been evaluated (the elimination of water molecules occurs from $T \geq 120\text{--}150^\circ\text{C}$; this process has been followed by IR spectroscopy). We obtained the following formula



The free energy of formation of the $(\text{H}_2\text{O})_{0.6}\text{Cu}_{0.2}\text{Ca}_{0.8}\text{CO}_3$ complex can, therefore, be determined from eq 4. We obtained $\Delta_f G^*[(\text{H}_2\text{O})_{0.6}\text{Cu}_{0.2}\text{Ca}_{0.8}\text{CO}_3] = -1147 \text{ kJ}$. This value is slightly lower than that for calcite ($\Delta_f G^*[\text{calcite}] = -1129 \text{ kJ}$), and thereby explains the relative stability of vaterite grains experimentally observed under the influence of Cu(II) in ultrapure water. An energetic diagram illustrating the free energies of formation of the different carbonates involved in the

crystalline transformation of vaterite under the influence of Cu(II) in ultrapure water is shown in Figure 4.

Dissolution/Degradation of Copper « Coatings ». Previous works^{11,24,30,31} have shown that information about the chemical environments of Cu(II) present in a crystalline solid matrix can be obtained by using the intensity ratio $I_{\text{sat}}/I_{\text{pp}}$ [where I_{sat} and I_{pp} are the intensities of the satellite peak and the principal peak, respectively, measured from the XPS spectrum of $\text{Cu}_{2p3/2}$ level of Cu(II)]. Thus, D'Huysser et al.²⁴ have indicated that the $I_{\text{sat}}/I_{\text{pp}}$ ratio is equal to 0.85 for a Cu(II) with a 4-fold coordination and decreases to 0.55 for a Cu(II) with a 6-fold coordination. In the case where the thermodynamic solubility product is minimum [$(\text{IAP})_{\text{min}} = 10^{-9}$ with mol% $\text{CuCO}_3 \cong 2.1$; see Figure 1], the $I_{\text{sat}}/I_{\text{pp}}$ ratio was measured versus reaction time on the XPS spectra of $\text{Cu}_{2p3/2}$ level for the recovered solid. Our investigations reveal that after a reaction time of 1 day, $I_{\text{sat}}/I_{\text{pp}}$ is equal to 0.78. This value indicates that Cu(II) ions are isolated on vaterite grains surfaces and are localized in sites with distorted octahedral symmetries and a « mean » coordination number of <6, in agreement with our ESR results reported in a previous work.⁹ However, the micro-Raman analysis of Cu^{2+} -vaterite specimens visualized by optical microscopy (Figure 5) shows only a specific band attributed to vaterite, but does not permit the detection of bands ascribed to « copper coatings », probably because of their low contents/thickness on the vaterite grains surfaces. A SEM microphotograph (Figure 6A) indicates no morphological change (which would be induced by Cu^{2+} ions) on the spherical micropellets of vaterite. The $I_{\text{sat}}/I_{\text{pp}}$ ratio decreases to 0.62 after a reaction time of 4 days, indicating that significant changes in the chemical environment of this metal are taking place due to the progressive dissolution of these « coatings ». Micro-Raman analyses of different randomly selected microparticles indicate the presence of calcite with a characteristic band at 1086 cm^{-1} (Figure 7), and SEM and optical microphotographs show clearly significant morphological change on the analyzed specimens (Figure 6B). Likewise, IR spectra (Figure 3) show (i) the disappearance of the broad IR band at ca. 3450 cm^{-1} [that is ascribed to water vibration in hydrated complexes; $(\text{H}_2\text{O})_{0.6}\text{Cu}_{0.2}\text{Ca}_{0.8}\text{CO}_3$], thus indicating unambiguously the decomposition of these « coatings »; and (ii) the appearance of a new band at 712 cm^{-1} attributed to calcite that is generated through the crystalline transformation of vaterite. All these findings further confirm the importance of the vaterite dissolution in water [which is, in this case, slowed by the action of Cu(II)] during the crystalline transformation of this metastable calcium carbonate into calcite. However, even if the

concentration of Cu(II) in interaction with vaterite is relatively high ($\sim 10^{-2}\text{ M}$), no characteristic Raman or IR bands ascribed to « copper coatings » had been detected. Indeed micro-Raman point-by-point analysis of the randomly chosen specimens on the surface of Cu^{2+} -vaterite solids had only revealed a disappearance of the vibrational bands attributed to vaterite followed by a progressive appearance of new Raman bands ascribed to cubic calcite, aragonite, and malachite (Figure 8). SEM micrographs exhibit clearly the presence of the above mentioned compounds (Figure 6C). All these findings suggest that vaterite transformation into cubic calcite is intimately related to the presence of malachite crystals (generated at the surface of vaterite grains) that constitute a separated phase apart from coatings present on the vaterite surface. On the other hand, a separated aragonite phase characterized by the Raman band at 207 cm^{-1} appears either alone or in the presence of malachite with a Raman band at 431 cm^{-1} . Therefore, aragonite is considered as an intermediate phase in the course of transformation of vaterite into cubic calcite.

Conclusion

In this paper, Cu(II) adsorption on vaterite surfaces in ultrapure water has been examined. By analyzing the liquid and solid phases recovered from Cu^{2+} -vaterite systems in ultrapure water, thermodynamic solubility products (IAP) were calculated. These investigations have revealed a significant decrease of the vaterite solubility due to the generation of « copper coatings » (that are apparently less soluble than vaterite) on vaterite grains. In addition, the IR study has proved the existence of O-H bands, either from hydroxyl ions or water molecules, in these coatings. These observations suggest that « copper coatings » might be better considered more as hydrated Cu(II) complexes; that is, $(\text{H}_2\text{O})_x\text{Cu}_x\text{Ca}_{1-x}\text{CO}_3$. The substantiation of this suggestion has required detailed spectroscopic (IR, Raman, XPS) and electron microscopic studies of solids recovered from Cu^{2+} -vaterite systems in ultrapure water. In addition, an approach for determining fundamental thermodynamic properties of these complexes has been described. Thus, the free energy of formation of such a solid solution has been evaluated, and found to be close to that of calcite, showing unambiguously the apparent stabilization of vaterite in the presence of Cu(II). However, it should be noted that when Cu^{2+} concentration increases strongly in the bulk (10^{-2} M), Cu(II) coatings cannot grow indefinitely on vaterite surfaces and, thereby, a new phase ascribed to malachite [$\text{Cu}_2(\text{OH})_2(\text{CO}_3)$] appears in the system. SEM and Raman microanalyses of recovered solids have allowed successful monitoring of the different steps of this process.

CM9803399

(30) D'Huysser, A.; Le Calonnec, D.; Lenglet, M.; Bonnelle, J. P.; Jorgensen, C. K. *Mater. Res. Bull.* **1984**, *19*, 1157.

(31) Bechara, R.; Aboukaïs, A.; Guelton, M.; D'Huysser, A.; Grimblot, J.; Bonnelle, J. P. *Spectrosc. Lett.* **1990**, *23*(10), 1237.